Available online at www.sciencedirect.com

SciVerse ScienceDirect

Ceramics International 39 (2013) 7007–7013

CERAMICS INTERNATIONAL

www.elsevier.com/locate/ceramint

Effect of triethanolamine on the electrophoretic deposition of hydroxyapatite nanoparticles in isopropanol

Morteza Farrokhi-Rad, Taghi Shahrabi*

Department of Materials Science & Engineering, Tarbiat Modares University, P.O. Box 14115-143, Tehran, Iran

Received 14 January 2013; received in revised form 13 February 2013; accepted 14 February 2013
Available online 4 March 2013

Abstract

Suspensions of hydroxyapatite (HA) nanoparticles were prepared in isopropanol and triethanolamine (TEA) was used as the dispersant. It was found that H^+TEA species generated by proton capturing from isopropanol are chemically adsorbed on HA nanoparticles via strong hydrogen bonding, enhancing their zeta potential and hence colloidal stability. Electrophoretic deposition was performed at 60 V for various durations. It was found that sticking parameter (*f* factor) decreases with TEA concentration due to the increase in the potential (electrical + chemical) difference at the interface of deposit and suspension. The wet density of deposits increased with the zeta potential of particles as well as deposition time, due to the time dependent rearrangement of particles within the deposit caused by electro-osmotic flow which is stronger when the zeta potential is higher. It was found that the coating deposited from the suspension with 4 mL/L TEA had the best corrosion resistance in Ringer's solution at 37.5 °C due to its fine, homogeneous and crack-free microstructure acting as a good barrier against the corrosive medium.

Keywords: D. Hydroxyapatite (HA) nanoparticles; Electrophoretic deposition (EPD); Isopropanol; Triethanolamine (TEA); Hydrogen bonding.

1. Introduction

Hydroxyapatite (HA: $Ca_{10}(PO_4)_6(OH)_2$) is the main inorganic constituent of human bone (60% Vol) [1]. HA has been used extensively in biomedical applications due to its high biocompatibility, bioactivity, biodegradability and osteoconductivity [2–4]. However, HA has poor mechanical properties such as low fracture toughness limiting its clinical applications; therefore HA has been widely used in the form of coating on the metallic implants such as titanium and 316L stainless steel. Several coating methods such as sol–gel [5,6], plasma spraying [7,8], sputtering [9], biomimetic formation [10] and so on have been successfully used to deposit HA coatings on metallic substrates. Electrophoretic deposition (EPD) is another method which has been used extensively to prepare HA coatings on metallic substrates in recent years [11–14] due to its advantages such as simplicity, low cost equipment, short formation times and possibilty of controling the microstructure and thickness of deposits by a simple adjustment of deposition parameters such as voltage and time [15]. Another important advantage of EPD is the possibility to prepare HA coatings with interconnected porosity essential for implant fixation by bone ingrowths into the pores [16]. The colloidal stability and the zeta potential of particles have a great influence on the kinetics of EPD as well as the quality of the obtained coatings. Using water as the solvent for suspension preparation is limited in EPD, due to its electrolysis at relatively low applied voltages [17]; so the non-aqueous solvents such as alcohols are usually used in EPD [18]. The zeta potential of particles is usually very low in non-aqueous solvents due to their low dielectric constant. The zeta potential and the colloidal stability of particles can be enhanced by the addition of an efficient dispersant into the non-aqueous suspensions. Triethanolamine (TEA) is an organic base which can be used as the dispersant to increase the zeta potential and colloidal stability of particles in non-aqueous suspensions [12,18]. In the present work the mechanism of TEA action as a dispersant for the suspension of HA nanoparticles in isopropanol as well as its effects on their EPD and the properties of obtained coatings have been investigated.

*Corresponding author. Tel.: +98 21 82883378.
E-mail addresses: morteza_farrokhi_rad@yahoo.com (M. Farrokhi-Rad), tshahrabi34@modares.ac.ir (T. Shahrabi).

0272-8842/$ - see front matter © 2013 Elsevier Ltd and Techna Group S.r.l. All rights reserved.
http://dx.doi.org/10.1016/j.ceramint.2013.02.038

2. Materials and method

2.1. Suspension preparation

Hydroxyapatite (HA) nanoparticles were synthesized by the Metathesis method [19]. Triethanolamine was added at different concentrations (0, 0.33, 1.33, 4, 8, 16.66, 33.33 and 66.66 mL/L) into the isopropanol and magnetically stirred for 15 min to homogenize the solutions. HA nanoparticles were added into the solutions (20 g/L), magnetically stirred for 24 h and ultrasonically dispersed for 10 min (Sonopuls HD 3200, 20 kHz; Bandelin Co., Berlin, Germany) to obtain the homogeneous suspensions. The electrical conductivity of the solutions and corresponding suspensions was measured against TEA concentration. The zeta potential of HA nanoparticles was measured against TEA concentration (Malvern instrument, Worcestershire, UK). The samples for zeta potential measurement were prepared by diluting the suspensions according to the method described in Ref. [18]. Fourier transform infrared spectroscopy (FTIR) was used to investigate the adsorption of TEA on HA nanoparticles. The samples for FTIR analysis were as synthesized HA nanopowder as well as the powder removed from the suspension with 4 mL/L TEA by centrifuging and washing the extracted powder with deionized water (2 times, 4000 rpm) and drying it at 120 °C for 24 h.

2.2. Electrophoretic deposition

The plates of 316L stainless steel with the dimensions of 20 mm × 40 mm × 1 mm were used as the substrate and counter electrodes. Only 4 cm^2 of substrates was exposed to deposition and remainder insulated. The distance between the electrodes was 1 cm in EPD cell. EPD was performed at 60 V for different durations (15, 30, 60, 120, 240 and 360 s) using a DC power supply (HY30002E; Huayi Electronics Industry Co., Hangzhou, Zhejiang, China). The wet weight (W_{wet}) of deposits was measured immediately after EPD (GR-200, A&D Co., Tokyo, Japan). The immersion weight of deposits (W_{im}) was recorded continuously and *in situ* according to the method described in Ref. [20]. During *in situ* deposition weight measurement, the voltage was applied for 6 min and then switched off for 6 min and then reapplied at a same magnitude but reversed polarity. The sticking parameter was calculated using the Hamaker equation as well as the method described in Ref. [20]. The wet density of deposits was calculated according to the following equation at different deposition times:

$$\rho_{wet} = \frac{W_{wet}}{Vol_{wet}} \quad \text{and} \quad Vol_{wet} = \frac{W_{wet} - W_{imm}}{\rho_{ISP}} \tag{1}$$

where Vol_{wet} is the wet volume of the deposit and ρ_{ISP} is the density of isopropanol (0.78 g. cm^{-3}).

The microstructure of deposits was observed by a scanning electron microscope (SEM). The coatings were dried at room temperature overnight and then sintered at 700 °C (heating rate 5 °C/min) for 1 h under flowing argon atmosphere (argon flow rate: 20 mL/min). The effect of HA coatings on the corrosion rate of substrate in Ringer's solution at 37.5 °C was studied by the potentiodynamic polarization technique (potentiostat/galvanostat Autolab 84367). A three electrode cell was used for potentiodynamic polarization studies; uncoated (bare substrate) and HA coated substrates were used as the working electrode; saturated calomel electrode (SCE) and a platinum wire mesh were used as the reference and counter electrodes, respectively (scan rate: 1 mV/s).

3. Results and discussion

3.1. Suspension properties

The electrical conductivities of the solutions and corresponding suspensions against TEA concentration are shown in Fig. 1. As can be seen the electrical conductivity of both the solution and suspension increases with TEA concentration. Also it can be seen that the conductivity of the suspensions is less than that of the solutions at the same concentration of TEA. The conductivity of isopropanol increases with TEA addition according to the following reaction:

$$ROH + TEA \Leftrightarrow RO^- + H^+TEA \tag{2}$$

When HA nanoparticles are added into the solution, the H^+TEA species generated through the reaction (2) are effectively adsorbed (see Fig. 3) on their surface resulting in the conductivity drop (since the mobility of charged particles is lower than that of free ions).

The zeta potential of HA nanoparticles *versus* TEA concentration is shown in Fig. 2. As can be seen the zeta potential increases with TEA concentration and reaches the maximum value at the TEA concentration of 4 mL/L and then decreases upon its further addition. As explained previously when HA nanoparticles are added into the solution of TEA in isopropanol, the H^+TEA species

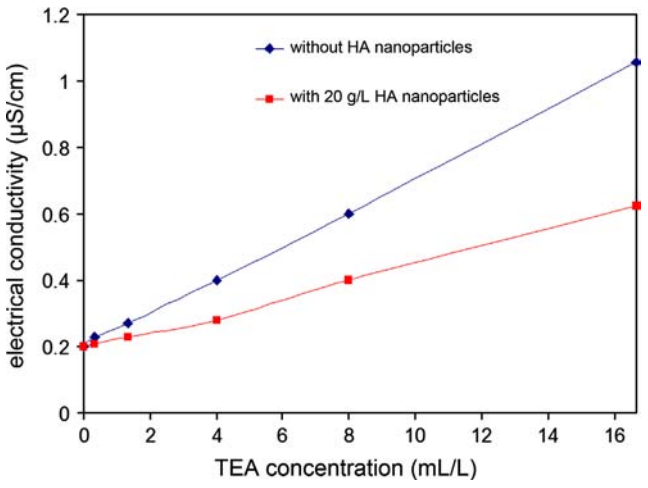

Fig. 1. Electrical conductivity of isopropanol and corresponding suspension against TEA concentration.

generated by reaction (2) are adsorbed on them and enhance their surface charge and so their zeta potential. It can be said that the effect of ionic strength increasing and so double layer thickness decreasing [21] becomes more prominent than H^+TEA adsorption at TEA concentrations more than 4 mL/L, resulting in zeta potential decline.

The results of FTIR analysis are shown in Fig. 3. It can be seen that in addition to the peaks that appeared in the spectra of the as synthesized HA nanopowder, the spectra of the powder removed from the suspension with 4 mL/L TEA show other peaks at 2875 and 2945 cm^{-1} attributed to the stretching vibration of C–H bond proving the H^+TEA as well as TEA adsorption on HA nanoparticles. Also it is seen that the peak at 3750 cm^{-1} belonging to the surface P–OH groups of HA [22] does not appear in the spectra of TEA adsorbed HA nanopowder. It can be concluded that the surface P–OH groups of HA act as the adsorption sites for TEA. As schematically shown in Fig. 4, TEA can chemically adsorb on the HA nanoparticles through strong hydrogen bonding with their surface P–OH groups. The adsorption of several other chemical compounds on HA through hydrogen bonding with its surface P–OH groups has been also reported in literature. Ishikawa [23] found that surface P–OH groups of HA act as the effective adsorption sites for H_2O, CO_2 and CH_3OH. Hidekazu et al. [24] found that pyridine, n-butylamine and acetic acid adsorb on HA through the hydrogen bonding with its surface P–OH groups.

3.2. Electrophoretic deposition

The electrical resistance of the deposits against EPD time is shown in Fig. 5. In our previous work [20] it was found that the electrical resistance of the titania deposits formed from the suspension with 0.33 mL/L TEA is considerably lower than that of those formed from the suspension without TEA. It was concluded that this is due to the detachment of some physically adsorbed H^+TEA from the surface of deposited titania nanoparticles under applied electric field resulting in the increased concentration of charge carriers in deposit decreasing its electrical resistance. However as can be seen in Fig. 5 at the same deposition time, the resistance of the HA deposit shaped

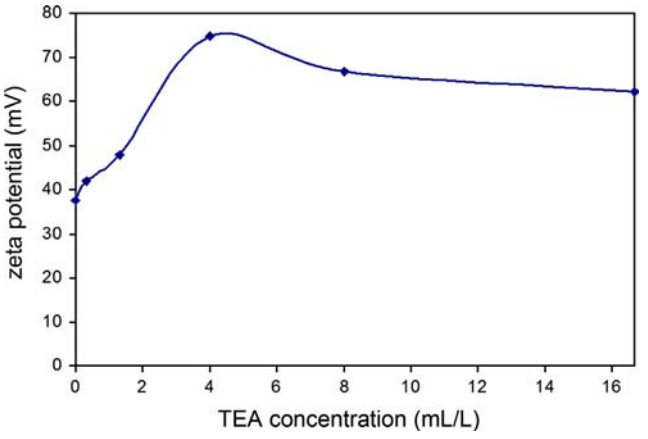

Fig. 2. Zeta potential of HA nanoparticles (20 g/L) against TEA concentration in isopropanol.

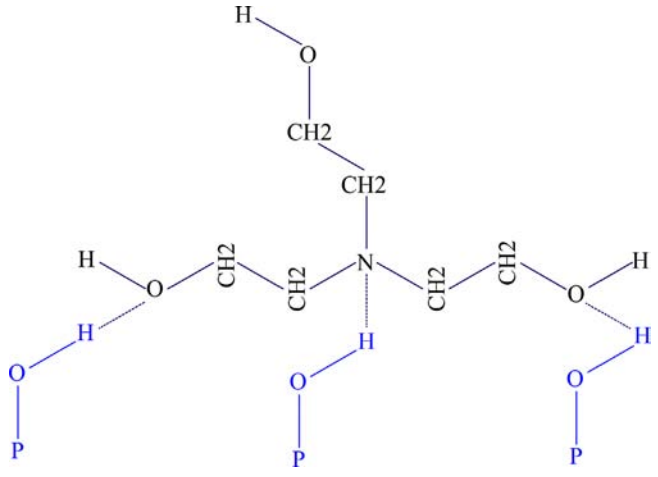

Fig. 4. Schematic representation of TEA adsorption on HA nanoparticles through hydrogen bonding with their surface P–OH groups.

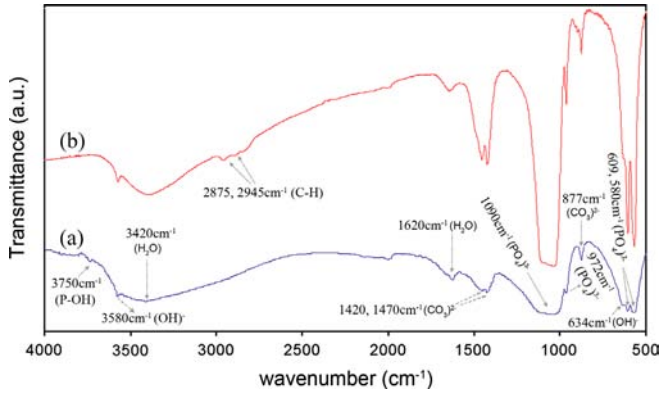

Fig. 3. FTIR spectra for (a) as synthesized HA nanopowder and (b) HA nanopowder removed from the suspension with 4 mL/L TEA.

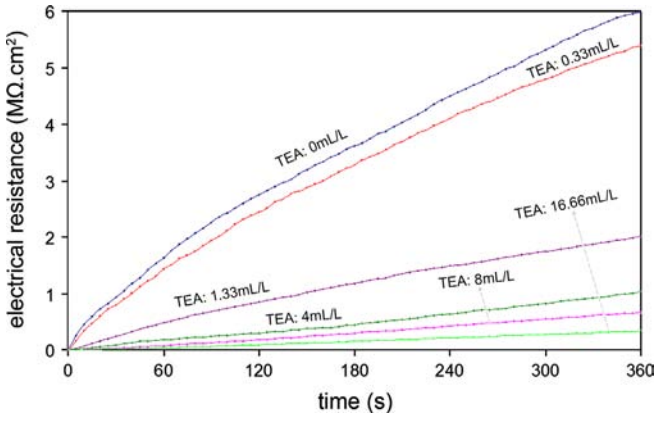

Fig. 5. Electrical resistance of the deposits formed at 60 V from the suspensions with different TEA concentrations *versus* time.

from the suspension with 0.33 mL/L TEA is only slightly less than that of deposit prepared from the suspension without TEA; so it can be concluded that H^+TEA (as well as TEA) species adsorb so strongly on HA nanoparticles that their detachment from particles surface does not occur under the applied electric fields conventional in EPD. As explained previously TEA is chemically adsorbed on the HA nanoparticles through the relatively strong hydrogen bonding with its surface P—OH groups.

The results for *in situ* measurement of deposition weight against time are shown in Fig. 6. A detailed explanation about typical trend of *in situ* weight plots against time is reported in our previous work [20]. In our previous work [20] it was observed that the rate of titania nanoparticles detachment from deposit into the suspension after voltage switch off is the fastest for one deposited from the suspension in which the zeta potential of titania nanoparticles is the highest (TEA: 0.33 mL/L). However, it can be seen in Fig. 6 that the rate of HA nanoparticles detachment after voltage switch off from the deposit into the suspension continuously increases with TEA concentration. As mentioned previously, TEA has a high affinity to adsorb on the HA nanoparticles surfaces. The amount of TEA adsorbed on HA nanoparticles increases continuously with increasing TEA concentration in the suspension. In fact both the electrical (due to the different concentrations of charged HA nanoparticles (or H^+TEA) at the interface of deposit and suspension) and chemical potential (due to the different concentrations of TEA at the interface of deposit and suspension) differences at the interface of deposit and suspension contribute to the particles instability and detachment there. Both the electrical and chemical potential differences increase at the interface with the addition of TEA up to 4 mL/L, where the zeta potential of HA nanoparticles is the maximum; so the rate of particles detachment increases with TEA concentration. The electrical potential difference decreases (due to the reduction in the zeta potential) while the chemical potential difference increases again with the TEA addition at concentrations higher than 4 mL/L. It can be concluded that the total potential difference (electrical+ chemical) increases continuously at the interface with TEA concentration so that the rate of particles detachment increases continuously with it. The results for *f* factor (sticking parameter) at initial times of EPD calculated by Hamaker equation and the method described in Ref. [20] *versus* TEA concentration are shown in Fig. 7. As can be seen the values of *f* factor obtained by Hamaker equation and the method described in Ref. [20] are in good agreement. The *f* factor decreases continuously with TEA concentration. As can be seen in Fig. 6 the deposition rate from the suspensions with 0, 0.33, 1.33 and 8 mL/L TEA is nearly equal, while it is expected that the deposition rate increases in the order: 0, 0.33, 1.33 and 8 mL/L TEA according to the experimental results obtained for electrophoretic mobility of HA nanoparticles. This can be explained by the results obtained for *f* factor: while the electrophoretic mobility of HA nanoparticles increases with TEA concentration the *f* factor decreases with it (the mobility of HA nanoparticles and *f* factor for the suspensions with 0, 0.33, 1.33 and 8 mL/L TEA are (0.323 μm.cm $(V\,s)^{-1}$ and 0.95), (0.362 μm.cm $(V.s)^{-1}$ and 0.85), (0.437 μm.cm $(V.s)^{-1}$ and 0.77) and (0.590 μm.cm $(V.s)^{-1}$ and 0.69), respectively). The deposition rate from the suspension with 4 mL/L TEA is the fastest due to the highest mobility of HA nanoparticles in it (0.645 μm.cm $(V.s)^{-1}$).

The wet density of deposits against EPD time is shown in Fig. 8. As can be seen the wet density increases with deposition time and attains a plateau at longer EPD times. Also it can be seen that the wet density increases with zeta potential at the same deposition time, so that the wet density of the deposit formed from the suspension with 4 mL/L TEA is the highest followed by those deposited from the ones with 8, 16.66, 1.33, 0.33 and 0 mL/L TEA. The increase in the wet density of deposits with time is due to the particles rearrangement within them caused by electro-osmotic flow around the deposited particles. The velocity of electro-osmotic flow can be determined by the following equation [18]:

$$v = \frac{\varepsilon_0 \varepsilon_r \zeta}{\eta} E_{dep} \tag{3}$$

where ζ is the zeta potential of particles, ε_0 is the permittivity of vacuum, ε_r is the relative dielectric constant

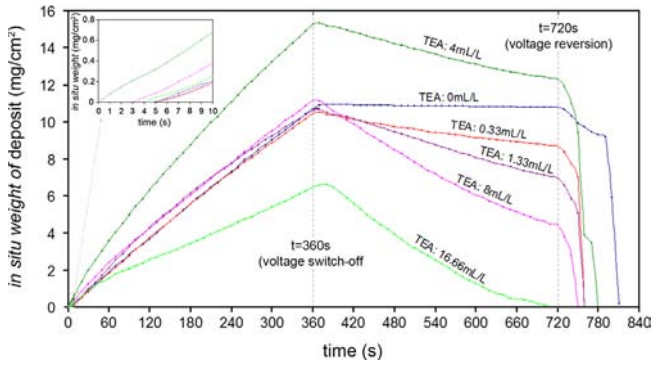

Fig. 6. *In situ* weight of deposits formed at 60 V from the suspensions with various concentrations of TEA against time.

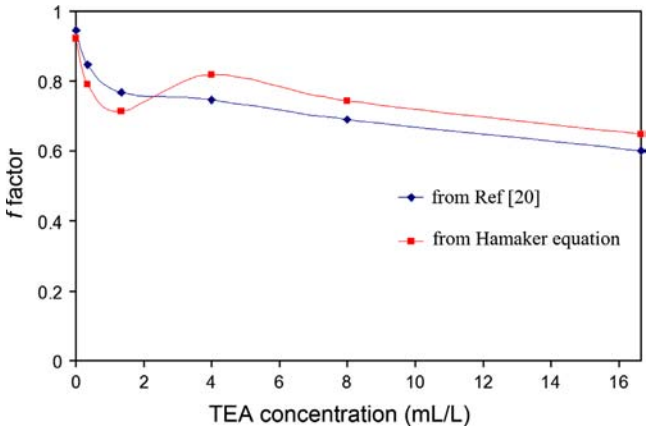

Fig. 7. Sticking parameter (*f* factor) calculated using Hamaker equation and method described in Ref. [20] against TEA concentration at 60 V and initial times of EPD.

of medium, η is the viscosity of medium and E_{dep} is the electric field over the deposit. The velocity of electro-osmotic flow increases with increasing the zeta potential of particles resulting in the intensive electro-osmotic flow and so the effective particles rearrangement within the deposit.

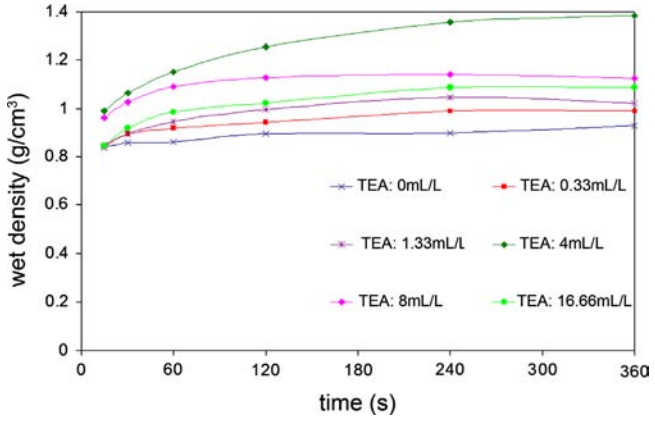

Fig. 8. Wet density of deposits formed at 60 V from the suspensions with various concentrations of TEA against time.

The optical microscope images of dried coatings deposited from the suspensions with the different concentrations of TEA are shown in Fig. 9. The coatings were deposited at 60 V and deposition time was selected so that the deposition weight becomes equal for all deposits (deposition times were 70, 80, 70, 40, 65 and 120 s for the suspensions with 0, 0.33, 1.33, 4, 8 and 16.66 mL/L TEA, respectively). As can be seen the coatings deposited from the suspensions with 0 and 0.33 mL/L TEA have the high concentrations of large cracks developed during drying. The coatings deposited from the suspensions with 1.33 and 16.66 mL/L TEA have a high concentration of smaller cracks. Cracking does not occur in the coatings deposited from the suspension with 4 mL/L TEA. Cracking occurs in electrophoretically deposited coatings due to the large drying shrinkages exerting mechanical stresses on them. The higher the wet density of deposit the lower the volume of liquid phase which should be removed during drying;

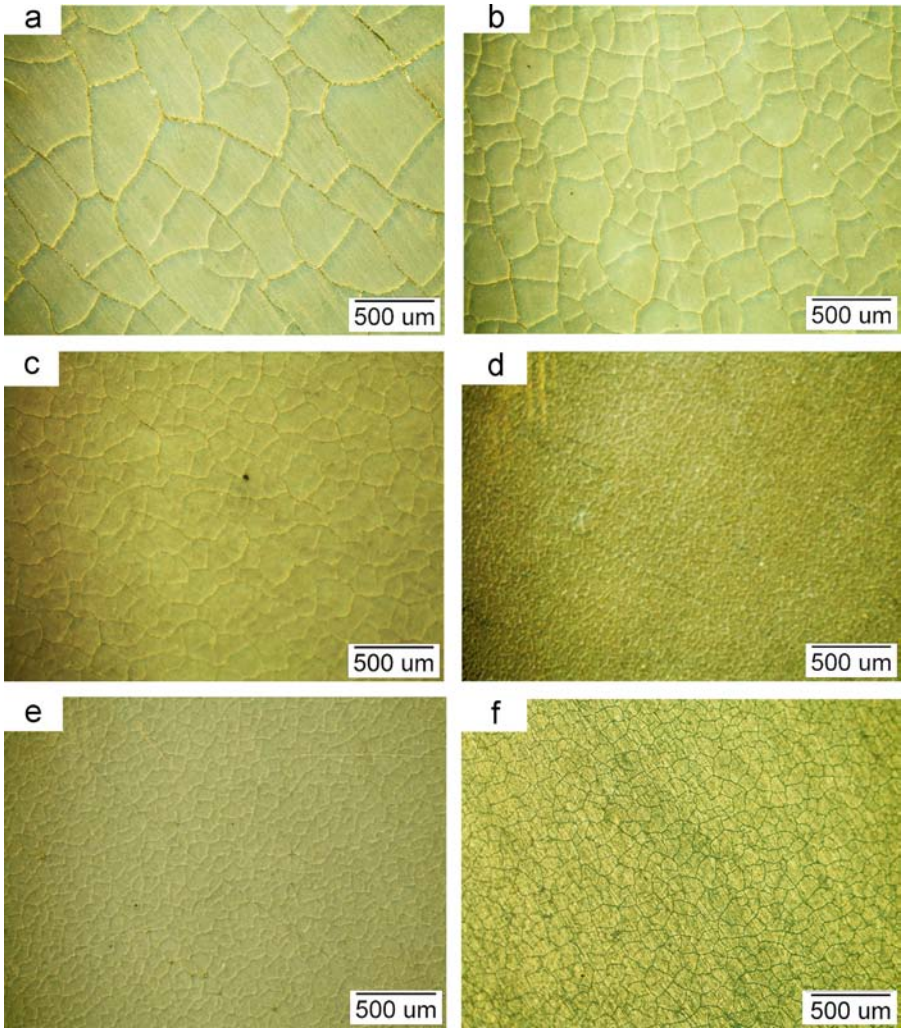

Fig. 9. Optical microscope images of coatings with the same weight deposited at 60 V from the suspensions with different concentrations of TEA: (a) 0, (b) 0.33, (c) 1.33, (d) 4, (e) 8 and (f) 16.66 mL/L (deposition times were 70, 80, 70, 40, 65 and 120 s for the suspensions with 0, 0.33, 1.33, 4, 8 and 16.66 mL/L TEA, respectively).

this results in smaller drying shrinkages for the deposits with higher wet densities and so smaller mechanical stresses exerted on them during drying. The wet density of the deposit formed from the suspension with 4 mL/L TEA is the highest, so the drying shrinkage and cracking is the lowest for it.

The SEM images of the coatings deposited at 60 V and 30 s from the suspensions with the different concentrations of TEA are shown in Fig. 10. As can be seen among the deposits, the one deposited from the suspension with 4 mL/L TEA has the best microstructure with fine particles and small number of fine agglomerates. However other deposits, especially those deposited from the suspensions with 0 and 0.33 mL/L, have uneven microstructures with coarse agglomerates. The zeta potential of HA nanoparticles is the highest (74.7 mV) in the suspension with 4 mL/L TEA; so the particles agglomeration is small in it due to the large repulsion electrostatic force between them.

The polarization curves for bare stainless steel substrate and those coated with HA at 60 V (nearly same thickness of HA coatings was deposited on all samples (the deposition times were the same as those used for the specimens of Fig. 9)) from the suspensions with different concentrations of TEA in Ringer's solution at 37.5 °C are shown in Fig. 11. The corrosion current density (i_{corr}) and potential (E_{corr}) extracted from these curves are summarized in Table 1. The corrosion rate of substrate decreases as it is coated with HA. Among the specimens, the one coated from the suspension with 4 mL/L TEA has the lowest i_{corr} and the highest E_{corr} and so the best corrosion resistance due to the fine, homogeneous and crack free microstructure of the coating deposited on it (Figs. 9 and 10). The cracks in the coatings deposited from the suspensions with 0, 1.33 and 16.66 mL/L TEA (Fig. 9) act as short diffusion paths for corrosive solution to reach the metal surface, resulting in their faster corrosion rates.

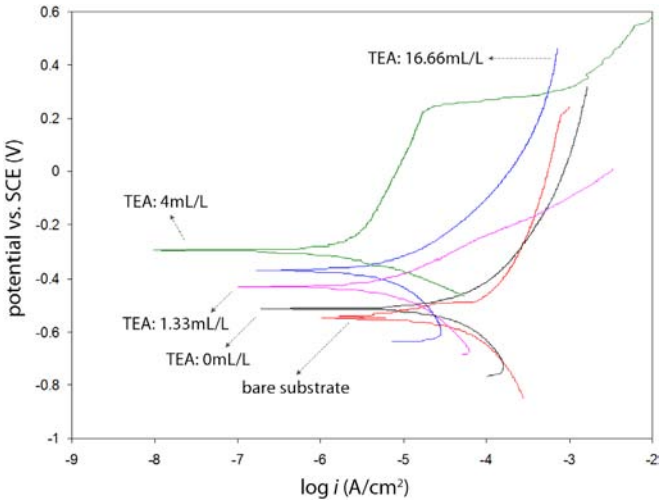

Fig. 11. Polarization curves for bare stainless steel substrate and those coated with HA at 60 V (nearly same thickness of HA coatings was deposited on all samples (the deposition times were the same as those used for the specimens of Fig. 9)) from the suspensions with different concentrations of TEA in Ringer's solution at 37.5 °C.

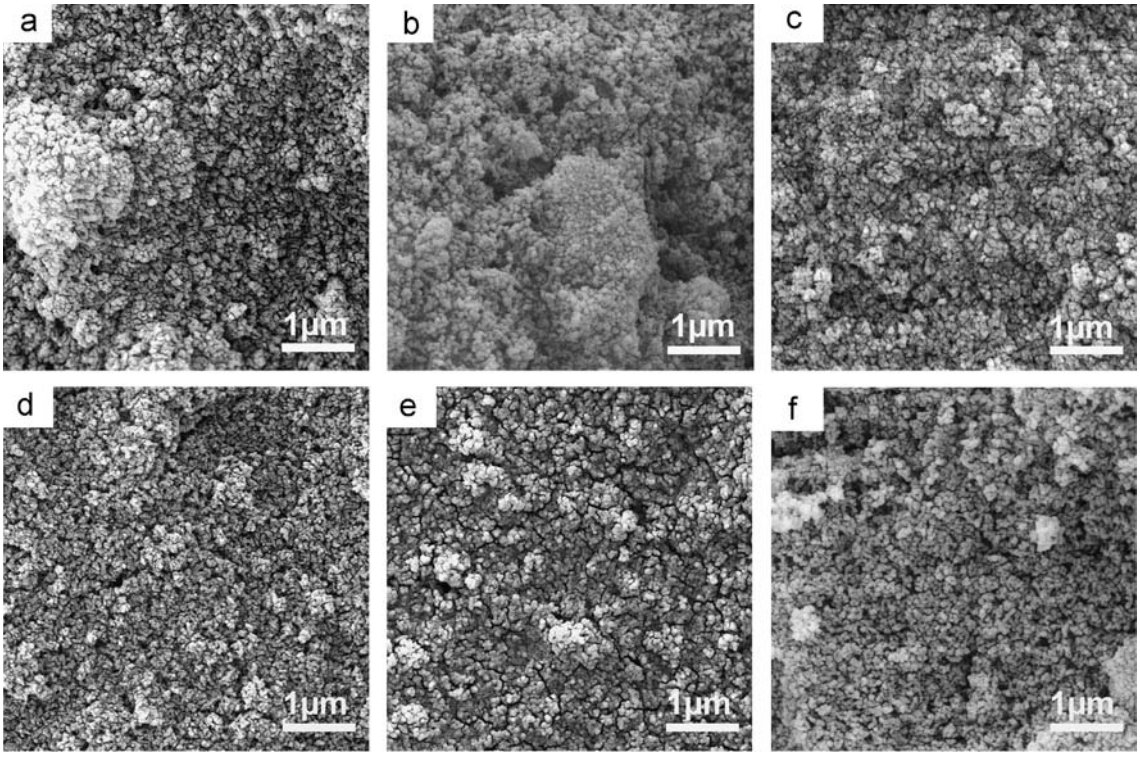

Fig. 10. SEM images of the coatings deposited at 60 V and 30 s from the suspensions with different concentrations of TEA: (a) 0, (b) 0.33, (c) 1.33, (d) 4, (e) 8 and (f) 16.66 mL/L.

Table 1
Corrosion current density (i_{corr}) and potential (E_{corr}) for bare stainless steel and substrates coated from the suspensions with different concentrations of TEA in Ringer's solution at 37.5 °C.

Specimen (mL/L)	E_{corr} (V)	I_{corr} (μA/cm^2)
Bare stainless steel	−0.546	30.33
TEA: 0	−0.513	19.93
TEA: 1.33	−0.433	5.40
TEA: 4	−0.295	2.20
TEA: 16.66	−0.371	3.11

4. Conclusions

It was found that H^+TEA as well as TEA species are chemically adsorbed on HA nanoparticles through strong hydrogen bonding with their surface P–OH groups, resulting in the increase in the zeta potential and colloidal stability of HA nanoparticles in the suspension. It was found that the sticking parameter (*f* factor) decreases with increasing TEA concentration in the suspension due to the increase in the potential (electrical + chemical) difference at the interface between deposit and suspension. The wet density of deposit increases with deposition time and zeta potential of particles due to the electro-osmotic flow around the particles within the deposit. The cracking due to the drying shrinkages was the lowest for the coating deposited from the suspension with 4 mL/L TEA due to its higher wet density resulting in smaller drying shrinkage. Also it was found that the coating deposited from the suspension with 4 mL/L TEA had the best corrosion resistance in Ringer's solution environment at 37.5 °C due to its fine, homogeneous and crack-free microstructure acting as a good barrier against corrosive medium.

References

[1] T.S.B. Narasaraju, D.E. Phebe, Review: Some physico-chemical aspects of hydroxylapatite, Journal of Materials Science 31 (1996) 1–21.

[2] J.M. Gomez-Vega, E. Saiz, A.P. Tomsia, G.W. Marshall, S.J. Marshall, Bioactive glass coatings with hydroxyapatite and Bioglass® particles on Ti-based implants. 1. Processing, Biomaterials 21 (2000) 105–111.

[3] P. Ducheyne, L.L. Hench, A. Kagan II, M. Martens, A. Bursens, J.C. Mulier, Effect of hydroxyapatite impregnation on skeletal bonding of porous coated implants, Journal of Biomedical Materials Research 14 (1980) 225–237.

[4] L.L. Hench, Bioceramics, Journal of the American Ceramic Society 81 (1998) 1705–1727.

[5] W. Weng, J.L. Baptista, Preparation and characterization of hydroxyapatite coatings on Ti6Al4V alloy by a sol–gel method, Journal of the American Ceramic Society 82 (1999) 27–32.

[6] D.-M. Liu, Q. Yang, T. Troczynski, Sol–gel hydroxyapatite coatings on stainless steel substrates, Biomaterials 23 (2002) 691–698.

[7] C.Y. Yang, B.C. Wang, E. Chang, J.D. Wu, The influences of plasma spraying parameters on the characteristics of hydroxyapatite coatings: A quantitative study, Journal of Materials Science: Materials in Medicine 6 (1995) 249–257.

[8] P. Cheang, K.A. Khor, Addressing processing problems associated with plasma spraying of hydroxyapatite coatings, Biomaterials 17 (1995) 537–544.

[9] T.G. Nieh, A.F. Jankowski, J. Koike, Processing and characterization of hydroxyapatite coatings on titanium produced by magnetron sputtering, Journal of Materials Research 16 (2001) 3238–3245.

[10] P. Habibovic, F. Barrère, C.A. Van Blitterswijk, K. De Groot, P. Layrolle, Biomimetic hydroxyapatite coating on metal implants, Journal of the American Ceramic Society 85 (2002) 517–522.

[11] I. Zhitomirsky, L. Gal-Or, Journal of Materials Science: Materials in Medicine 8 (4) (1997) 213–219;
C.T. Kwok, P.K. Wong, F.T. Cheng, H.C. Man, Characterization and corrosion behavior of hydroxyapatite coatings on Ti6Al4V fabricated by electrophoretic deposition, Applied Surface Science 255 (2009) 6736–6744.

[12] X.F. Xiao, R.F. Liu, Effect of suspension stability on electrophoretic deposition of hydroxyapatite coatings, Materials Letters 60 (2006) 2627–2632.

[13] M. Wei, A.J. Ruys, B.K. Milthorpe, C.C. Sorrell, Solution ripening of hydroxyapatite nanoparticles: Effects on electrophoretic deposition, Journal of Biomedical Materials Research 45 (1999) 11–19.

[14] M. Wei, A.J. Ruys, B.K. Milthorpe, C.C. Sorrell, J.H. Evans, Electrophoretic deposition of hydroxyapatite coatings on metal substrates: A nanoparticulate dual-coating approach, Journal of Sol–Gel Science and Technology 21 (2001) 39–48.

[15] L. Besra, M. Liu, A Review on fundamental and applications of electrophoretic deposition, Progress in Materials Science 52 (2007) 1–61.

[16] J. Ma, C. Wang, K.W. Peng, Electrophoretic deposition of porous hydroxyapatite scaffold, Biomaterials 24 (2003) 3505–3510.

[17] T. Uchikoshi, K. Ozawa, B.D. Hatton, and Y. Sakka, Electrophoretic deposition of alumina suspension in a strong magnetic field, Journal of Materials Research, 16 (2001) 321–324.

[18] M. Farrokhi-Rad, M. Ghorbani, Electrophoretic deposition of titania nanoparticles in different alcohols: Kinetics of deposition, Journal of the American Ceramic Society 94 (2011) 2354–2361.

[19] M. Wei, A.J. Ruys, B.K. Milthorpe, C.C. Sorrell, Precipitation of hydroxyapatite nanoparticles: Effects of precipitation method on electrophoretic deposition, Journal of Materials Science: Materials in Medicine 16 (2005) 319–324.

[20] M. Farrokhi-Rad, T. Shahrabi, Electrophoretic deposition of titania nanoparticles: Sticking parameter determination by an *in-situ* study of the EPD kinetics, Journal of the American Ceramic Society 95 (2012) 3434–3440.

[21] S.G.J. Heijman, H.N. Stein, Electrostatic and sterical stabilization of TiO2 dispersions, Langmuir 11 (1995) 422–427.

[22] Z.H. Cheng, A. Yasukawa, K. Kandori, T. Ishikawa, FTIR study of adsorption of CO2 on nonstoichiometric calcium hydroxyapatite, Langmuir 14 (1998) 6681–6686.

[23] T. Ishikawa, Surface structure and molecular adsorption of apatites, Studies in Surface Science and Catalysis 99 (1996) 301–318.

[24] H. Tanaka, T. Watanabe, M. Chikazawa, FTIR and TPD studies on the adsorption of pyridine, n-butylamine and acetic acid on calcium hydroxyapatite, Journal of the Chemical Society—Faraday Transactions 93 (1997) 4377–4381.